Effects of Growth Temperature on Carbon Nanotube Array Thermal Interfaces

Baratunde A. Cola

Placidus B. Amama

Xianfan Xu

Timothy S. Fisher
e-mail: tsfisher@purdue.edu

School of Mechanical Engineering and Birck Nanotechnology Center,
Purdue University,
West Lafayette, IN 47907

Due to their excellent compliance and high thermal conductivity, dry carbon nanotube (CNT) array interfaces are promising candidates to address the thermal management needs of power dense microelectronic components and devices. However, typical CNT growth temperatures (~800°C) limit the substrates available for direct CNT synthesis. A microwave plasma chemical vapor deposition and a shielded growth technique were used to synthesize CNT arrays at various temperatures on silicon wafers. Measured growth surface temperatures ranged from 500°C to 800°C. The room-temperature thermal resistances of interfaces created by placing the CNT covered wafers in contact with silver foil (silicon-CNT-silver) were measured using a photoacoustic technique to range from approximately 7 $mm^2°C/W$ to 19 $mm^2°C/W$ at moderate pressures. Thermal resistances increased as CNT array growth temperature decreased primarily due to a reduction in the average diameter of CNTs in the arrays.
[DOI: 10.1115/1.2969758]

Keywords: carbon nanotube, thermal interface material, contact thermal resistance, plasma CVD, low temperature, photoacoustic

Introduction

As semiconductor technology continues to advance, resulting in progressive reductions of device feature sizes and expansion of application opportunities, ensuring reliable operation has become a growing challenge. The effective and efficient transfer of heat from a chip to a heat sink is a vital step in meeting this challenge. Advanced thermal management schemes that employ carbon nanotube (CNT) arrays as interface materials have been suggested as a means to dissipate high heat fluxes while maintaining low chip temperatures [1–6]. Under moderate pressure, CNT array interfaces have been reported to produce thermal resistances as low as 8 $mm^2°C/W$ for arrays grown on one side of the interface [6] and as low as 4 $mm^2°C/W$ for arrays grown on both sides of the interface [4]. However, the temperatures at which these CNT array thermal interfaces were grown (>800°C) are incompatible with the temperature-sensitive substrates used in standard semiconductor processes because the electrical performance of most metal contacts and interconnects degrades when exposed to temperatures up to 450°C for more than a limited time [7].

Contributed by the Heat Transfer Division of ASME for publication in the JOURNAL OF HEAT TRANSFER. Manuscript received July 6, 2007; final manuscript received June 17, 2008; published online September 2, 2008. Review conducted by Yogendra Joshi.

An insertable CNT array/foil material was recently suggested as a way to apply CNT arrays to an interface without exposing the mating materials to normal CNT growth temperatures, and resistances as low as 10 $mm^2°C/W$ were achieved under moderate pressure [5]. While this technique seems promising, progress in low-temperature synthesis has been reported [7–10], and these approaches may prove advantageous for their ability to offer seamless integration into existing manufacturing processes; yet, to the best of our knowledge, the literature reveals no studies on the effects of decreased growth temperature on the thermal performance of CNT array interfaces. In this Technical Brief, we report on studies of thermal conduction through CNT array interfaces grown at various temperatures, lower than those previously reported.

Experimental Methods

Sample Fabrication. Microwave plasma chemical vapor deposition (MPCVD) [11] and a shielded growth technique [10] were used to synthesize vertically oriented CNT arrays on polished silicon wafers (560 μm thick). Iron oxide (Fe_2O_3) nanoparticles were deposited as a catalyst via a dendrimer template [12] on a 30 nm titanium barrier layer deposited atop the silicon. The silicon wafers were elevated (catalyst side facing away from the plasma) on a 5.5 mm thick molybdenum puck by 1.2 mm thick ceramic spacers, and the puck was set in the growth chamber on a heated stage, as illustrated in Fig. 1. The stage temperature, T_{stage}, was set to 800°C, 700°C, 600°C, 500°C, 400°C, 300°C, and 200°C for different synthesis processes, and the catalyst was heated in nitrogen ambient. The plasma power ranged 400–500 W, and the growth chamber's pressure was 10 Torr. The MPCVD process gases were hydrogen (50 SCCM (SCCM denotes cubic centimeter per minute at STP)) and methane (10 SCCM), and growth was carried out for 20 min. Two separate runs were performed at each growth condition to test repeatability. A dual-wavelength pyrometer was aimed at the backside of the silicon wafers to measure their temperature, $T_{pyrometer}$, during growth and to quantify the significance of additional heating due to the plasma [13]. Because of the relatively low intrinsic thermal resistance of the silicon wafers, we expect the temperature at the catalytic surfaces to be nearer $T_{pyrometer}$ than to T_{stage}. Thus, we will refer to $T_{pyrometer}$ as the "growth temperature."

Sample Characterization. Figure 2 shows the scanning electron microscope (SEM) images that illustrate the results of CNT arrays grown at different temperatures. Figure 2(*a*) shows a vertically oriented CNT array grown at 806°C. Figures 2(*b*)–2(*h*) are SEM images of equal magnification that illustrate the CNT morphologies obtained from growth at 806–506°C, respectively. The CNTs in each sample were entangled near their free ends; yet, as illustrated in Fig. 2(*a*) and in the insets of Figs. 2(*c*)–2(*h*), the bulk of all CNT array samples were vertically oriented. A transmission electron microscope (TEM) was used to examine wall structure and revealed that nanotubes (as apposed to nanofibers) were grown at each temperature. The bottom inset in Fig. 2(*h*) contains a TEM image of a CNT grown at 506°C. Table 1 summarizes the morphological characteristics of the CNT arrays grown at each temperature. The data are characteristic of the CNT arrays produced from two growth experiments at each temperature; hence, redundant sample types were morphologically similar.

Raman spectroscopy was also used to characterize the CNT arrays grown at each temperature. Well defined *G* (indicating well ordered graphite) and *D* (indicating amorphous carbon and/or tube defects) bands were observed, and the band intensity ratios I_G/I_D were approximately 0.5 for each sample, indicating a similar quality of CNTs produced in this study. These results were somewhat unexpected, as the quality of CNTs can depend strongly on growth temperature; however, using the dendrimer-assisted catalysis technique, such control over CNT characteristics has been demon-

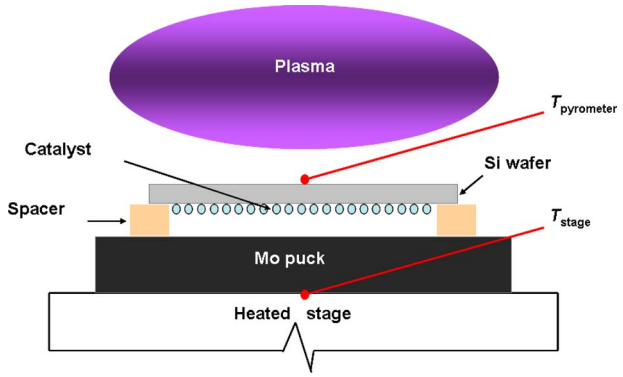

Fig. 1 Schematic of the sample configuration in the MPCVD chamber (not to scale)

strated in arrays grown at various temperatures [6,9].

The CNT diameter ranges displayed in Table 1 include two standard deviations from the mean, and the average is determined from diameters within the ranges. As growth temperature decreased, the CNT diameters decreased as expected because of the decrease in the mobility and/or aggregation of the catalyst nanoparticles [14]. For each sample, SEM images were analyzed to determine the density of CNTs by counting the number of CNTs per unit area. The mean CNT array heights were also estimated from SEM images. As growth temperature decreased, CNT density slightly decreased and mean array height decreased presumably because of a lower reaction energy that impedes the CNT growth process. At low growth temperatures, there is a decrease in surface diffusion of the catalyst nanoparticles, carbon solubility in the catalyst nanoparticles, and the diffusion of the carbon feedstock. All these factors play key roles during CNT growth especially the diffusion of carbon in the catalyst nanoparticles, which has been widely suggested as the rate-determining step.

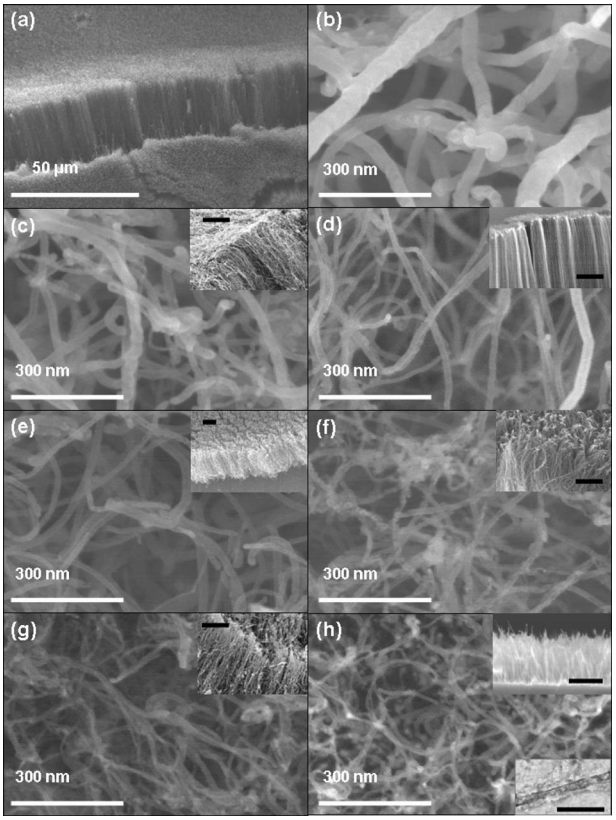

Fig. 2 SEM images of CNT arrays grown from 806°C to 506°C. (*a*) Vertically oriented CNT array grown at 806°C. (*b*) Higher magnification image of CNTs grown at 806°C. (*c*) CNTs grown at 737°C. The inset contains a lower magnification image that illustrates vertically oriented CNTs (scale bar is 5 μm). (*d*) CNTs grown at 707°C. The inset contains a lower magnification image (scale bar is 5 μm). (*e*) CNTs grown at 641°C (inset scale bar is 5 μm). (*f*) CNTs grown at 612°C (inset scale bar is 1 μm). (*g*) CNTs grown at 524°C (inset scale bar is 1 μm). (*h*) CNTs grown at 506°C. The top inset scale bar is 1 μm. The bottom inset contains a TEM image of a nanotube grown at 506°C (scale bar is 100 nm).

Thermal Resistance Measurement. The room-temperature thermal resistances of silicon-CNT-silver interfaces grown via MPCVD in the temperature range 806–506°C have been measured using a photoacoustic (PA) technique described in detail by Cola et al. [4]. Due to its transient nature, the PA technique can be used to measure multiple interface resistances as well as thermal diffusivity within layered materials such as CNT array interfaces [4]. The PA measurements were performed as a function of pressure in a range applicable to the thermal management of microprocessors, and relatively smooth silver foil (average peak-to-valley surface height of 0.4 μm) was used as the top interface substrate to enable precise PA measurements [4].

Results and Discussion

The average results from several PA measurements on each CNT array sample are illustrated in Fig. 3. Two separate samples were fabricated at each growth temperature and thermally tested. Figure 3 reveals exceptional consistency, both in terms of the repeatability of redundant samples and in terms of trends with respect to incremental variations in growth conditions. In fact, the thermal resistance values of the redundant samples significantly overlap considering the range of measurement uncertainty (± 0.5 mm^2°C/W). After testing, the interfaces were separated, and the CNTs remained well adhered to the silicon for each array, independent of growth temperature. The one-sided CNT array total thermal interface resistances R measured in this study are the sum of two local resistances (at the silicon-CNT interface and at the free CNT tip-silver interface) plus the intrinsic resistance of the CNT array. However, the local thermal resistances at the silicon-CNT interfaces were measured using the PA technique to be less than 1 mm^2°C/W and the resistances at the free CNT tip interfaces were measured to be approximately equal to the thermal resistances of the entire CNT array interface. Consequently, the contact of the CNTs to their growth substrate and the effective thermal conductivity of the CNT arrays had negligible effects on the total thermal resistances. Previous works [3,4] have also demonstrated that the thermal resistance at the interface to the free CNT tips dominates the resistance of one-sided CNT array interfaces.

As clearly illustrated in Fig. 3, the total thermal resistance R of the CNT array interfaces increases as CNT growth temperature decreases. We attribute this performance characteristic to the CNT array morphologies produced at different growth temperatures. As the growth temperature was decreased, the associated decreases in CNT density and average CNT diameter resulted in increased thermal resistance at the interface. Because the average peak-to-valley surface height of the silver foil (0.4 μm) is much less than the CNT array heights, we expect the variations in array height to have little effect on thermal resistance in this study [2]. For the most part, the CNT density and diameter changed simultaneously as array growth temperature changed; therefore, it is difficult to isolate the individual effects of these morphological characteristics on the associated changes in thermal interface resistance. However, the CNT densities varied by a much lesser percentage than the CNT diameters. Thus, we postulate that the changes in CNT diameter governed the changes in thermal resistance. This

Table 1 CNT morphologies for arrays grown at different temperatures

T_{stage} (°C)	800	700	600	500	400	300	200
$T_{pyrometer}$ (°C)	806	737	707	641	612	524	506
Plasma power (W)	400	400	400	500	500	500	500
Mean CNT array height (μm)	25	20	20	10	7	3	2
CNT density (%)	40–50	40–50	35–50	35–45	30–45	30–45	30–40
CNT diameter range (nm)	20–60	15–40	10–30	10–25	10–20	5–15	5–10
Average CNT diameter (nm)	40	30	23	15	15	10	8

performance characteristic is best illustrated through closer examination of the growth temperature ranges 641–524°C and 806–737°C, where the effects of CNT diameter are clearly distinguished.

When the CNT array growth temperature was reduced from 641°C to 612°C, the CNT density was slightly reduced, yet the average CNT diameter remained constant. As illustrated in Fig. 3, the thermal resistances produced by the 612°C arrays were approximately the same as the resistances produced by the 641°C arrays. When the growth temperature was reduced from 612°C to 524°C, the average CNT diameter in the arrays decreased from approximately 15 nm to 10 nm, yet the CNT density was approximately the same. In this case, the thermal resistances produced by the 524°C arrays were larger than the resistances produced by the 612°C arrays (Fig. 3). Additionally, when growth temperature was reduced from 806°C to 737°C, the average CNT diameter reduced while CNT density was approximately unchanged, and as illustrated in Fig. 3, interface resistance increased from the 806°C arrays to the 737°C arrays. These results are in support of the CNT array's average diameter having the dominate effect on the measured thermal resistances in this study.

Because the local resistances at the free CNT end dominates the total thermal resistances of the CNT array interface, changes in total resistance are due to changes in resistance at the free CNT end interface. At this interface, the characteristic contact size established between an individual CNT and the opposing silver substrate is at least an order of magnitude less than the room-temperature phonon mean free path of CNTs (approximately 150 nm [15]). Therefore, phonon transport through the contacts is ballistic [16,17], and the total thermal resistance at the free CNT ends interface, i.e., the total thermal resistance of the one-sided CNT array interface, can be represented as

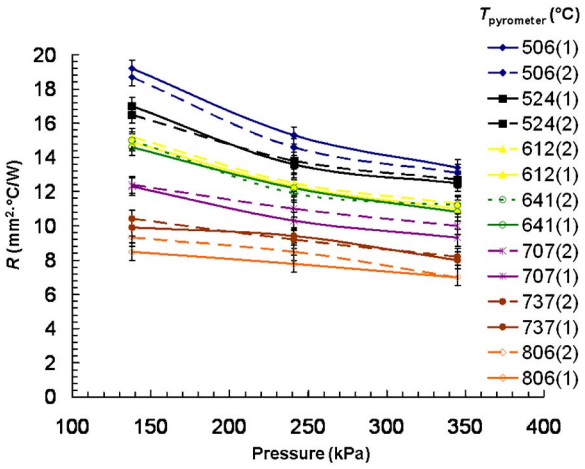

Fig. 3 Total thermal resistance *R* as a function of pressure for one-sided CNT array interfaces with arrays grown at various temperatures

$$R = R_b \cdot \frac{A}{A_r} \tag{1}$$

where R_b is the thermal resistance at individual CNT contacts, A_r is the real contact area established at the free CNT ends interface, and A is the apparent contact area. We postulate that changes in CNT diameter result in changes in A_r, which affects the total thermal resistance. Moreover, for the arrays in this study, we suggest that CNT diameter affects A_r primarily by influencing the effective hardness of the CNT array, which determines the number of CNTs that make contact with the opposing substrate. CNT coverage in this study only varied by a small percentage; consequently, as CNT diameter decreased, the total number of CNTs in the arrays increased. Hence, the smaller diameter CNTs were more closely packed (see Fig. 2). Presumably, as the smaller diameter CNT arrays deformed in the interface under the applied load, the close packing of CNTs promoted more tube-to-tube contact within the arrays, providing increased support for individual CNTs, such that the effective hardness of the arrays was increased and A_r was decreased, which is expected from traditional contact theory in which A_r is inversely proportional to hardness [18]. Therefore, as represented in Eq. (1), the total thermal resistance of the CNT array interfaces increases as A_r decreases.

Conclusions

The thermal resistances of CNT array interfaces grown in the temperature range 806–506°C were measured to range from 7 mm^2°C/W to 19 mm^2°C/W, respectively. These values comparable favorably to previously reported CNT array thermal interface resistances [1–6]. Moreover, it has been demonstrated that CNT arrays that provide good thermal interface conductance can be grown at reduced temperatures that allow integration with sensitive substrates (e.g., aluminum) that may be of particular interest to the heat transfer community. Thermal resistance was measured to increase as CNT array growth temperature decreased presumably due to an increase in the stiffness of the CNT arrays that reduced the amount of real contact area established in the interface. Further experiments and extensive modeling are still required to fully understand the contact mechanics in and the thermal transport through CNT array interfaces.

Acknowledgment

We gratefully acknowledge financial support from the National Science Foundation under grant CBET-0646015. The lead author is grateful for personal support from the Intel Foundation and the Purdue University Graduate School.

Nomenclature

A = apparent contact area, m^2
A_r = real contact area at the free CNT end interface, m^2
I_D = intensity of D band, a.u.
I_G = intensity of G band, a.u.
R = total thermal resistance of CNT array interface, mm^2°C/W

R_b = thermal resistance at individual CNT contacts, $mm^2 \cdot °C/W$

$T_{pyrometer}$ = temperature of silicon surface facing the plasma, °C

T_{stage} = temperature of the growth stage, °C

References

[1] Xu, J., and Fisher, T. S., 2006, "Enhanced Thermal Contact Conductance Using Carbon Nanotube Array Interfaces," IEEE Trans. Compon. Packag. Technol., **29**(2), pp. 261–267.

[2] Xu, J., and Fisher, T. S., 2006, "Enhancement of Thermal Interface Materials With Carbon Nanotube Arrays," Int. J. Heat Mass Transfer, **49**, pp. 1658–1666.

[3] Tong, T., Zhao, Y., Delzeit, L., Kashani, A., Meyyappan, M., and Majumdar, A., 2007, "Dense Vertically Aligned Multiwalled Carbon Nanotube Arrays as Thermal Interface Materials," IEEE Trans. Compon. Packag. Technol., **30**(1), pp. 92–100.

[4] Cola, B. A., Xu, J., Cheng, C., Hu, H., Xu, X., and Fisher, T. S., 2007, "Photoacoustic Characterization of Carbon Nanotube Array Thermal Interfaces," J. Appl. Phys., **101**, p. 054313.

[5] Cola, B. A., Xu, X., and Fisher, T. S., 2007, "Increased Real Contact in Thermal Interfaces: A Carbon Nanotube/Foil Material," Appl. Phys. Lett., **90**, p. 093513.

[6] Amama, P. B., Cola, B. A., Sands, T. D., Xu, X., and Fisher, T. S., 2007, "Dendrimer-Assisted Controlled Growth of Carbon Nanotubes for Enhanced Thermal Interface Conductance," Nanotechnology, **18**, p. 385303.

[7] Melechko, A. V., Merkulov, V. I., McKnight, T. E., Guillorn, M. A., Klein, K. L., Lowndes, D. H., and Simpson, M. L., 2005, "Vertically Aligned Carbon Nanofibers and Related Structures: Controlled Synthesis and Directed Assembly," J. Appl. Phys., **97**, p. 041301.

[8] Boskovic, B. O., Stolojan, V., Khan, R. U. A., Haq, S., and Silva, S. R. P., 2002, "Large-Area Synthesis of Carbon Nanofibers at Room Temperature," Nat. Mater., **1**, pp. 165–168.

[9] Hofmann, S., Ducati, C., Robertson, J., and Kleinsorge, B., 2003, "Low-Temperature Growth of Carbon Nanotubes by Plasma-Enhanced Chemical Vapor Deposition," Appl. Phys. Lett., **83**(1), pp. 135–137.

[10] Amama, P. B., Ogebule, O., Maschmann, M. R., Sands, T. D., and Fisher, T. S., 2006, "Dendrimer-Assisted Low-Temperature Growth of Carbon Nanotubes by Plasma-Enhanced Chemical Vapor Deposition," Chem. Commun. (Cambridge), **27**, pp. 2899–2901.

[11] Maschmann, M. R., Amama, P. B., Goyal, A., Iqbal, Z., Gat, R., and Fisher, T. S., 2006, "Parametric Study of Synthesis Conditions in Plasma-Enhanced CVD of High-Quality Single-Walled Carbon Nanotubes," Carbon, **44**, pp. 10–18.

[12] Amama, P. B., Maschmann, M. R., Fisher, T. S., and Sands, T. D., 2006, "Dendrimer-Templated Fe Nanoparticles for the Growth of Single-Wall Carbon Nanotubes by Plasma-Enhanced CVD," J. Phys. Chem. B, **110**, pp. 10636–10644.

[13] Teo, K. B. K., Hash, D. B., Lacerda, R. G., Rupesinghe, N. L., Bell, M. S., Dalal, S. H., Bose, D., Govindan, T. R., Cruden, B. A., Chhowalla, M., Amaratunga, G. A. J., Meyyappan, M., and Milne, W. I., 2004, "The Significance of Plasma Heating in Carbon Nanotube and Nanofiber Growth," Nano Lett., **4**(5), pp. 921–926.

[14] Meyyappan, M., Delzeit, L., Cassell, A., and Hash, D., 2003, "Carbon Nanotube Growth by PECVD: A Review," Plasma Sources Sci. Technol., **12**, pp. 205–216.

[15] Shi, L., 2001, "Mesoscopic Thermophysical Measurements of Microstructures and Carbon Nanotubes," Ph.D. thesis, University of California, Berkeley.

[16] Prasher, R., 2008, "Thermal Boundary Resistance and Thermal Conductivity of Multiwalled Carbon Nanotubes," Phys. Rev. B, **77**, 075424.

[17] Prasher, R., 2005, "Predicting the Thermal Resistance of Nanosized Constrictions," Nano Lett., **5**(11), pp. 2155–2159.

[18] Madhusudana, C. V., 1996, *Thermal Contact Conductance*, Springer-Verlag, New York.